Canadian Geotechnical Journal
April 2010, Volume 47, Number 4, pp. 486-496
http://dx.doi.org/10.1139/Z

Investigation of a possible submarine landslide at the Var delta front (Nice slope - SE France)

N. Sultan[1, *], B Savoye[1], G. Jouet[1], D. Leynaud[1], P. Cochonat[1], P. Henry[2], S. Stegmann[1] and A. Kopf[3]

[1] IFREMER, Département Géosciences Marines, France.
[2] CEREGE, Chaire de géodynamique du Collège de France, France.
[3] Department of Earth Sciences, University of Bremen, Germany.

*: Corresponding author : Nabil Sultan, Phone: +33298224259, Fax: +33298224570, email address : nabil.sultan@ifremer.fr

Abstract:

The Var prodelta progrades across a straight narrow shelf (less than 2 km wide) with a very steep continental slope reaching locally more than 30 degrees. Historically, the Var delta front is sadly famous for the 1979 catastrophic submarine landslide which results in several casualties and infrastructural damage. Geotechnical and geophysical investigations carried out in late 2007 to the East of the 1979 landslide scar provide evidence for the possible occurrence of a new important sedimentary collapse and submarine landslide. Geophysical data acquired in the area show the presence of several seafloor morphological steps rooted to shallow sub-surface seismic reflections. Moreover, in situ piezocone measurements demonstrate the presence of several shear zones at the border of the shelf break at different depth below the seafloor. The aim of this technical note is to present and discuss acquired geotechnical and geophysical data in terms of failure mechanisms and submarine landslides. Both geophysical and geotechnical data suggest the start-up of a progressive failure mechanism and reveal the possible occurrence of submarine landslide and the urgent need for mitigation procedures.

Keywords: CPTu, Gassy Soil, Piezocone, Shear zone, Submarine landslides.

1. Introduction

In 1979, a catastrophic event affected the Var prodelta and the Nice continental slope (Figure 1) where a part of the harbour constructed at the edge of the International Airport of Nice collapsed into the sea resulting in several casualties and infrastructural damage. An official technical report (Seed at al. 1988) following the 1979 event attributes the accident to a tsunami wave which was generated by a massive deep submarine landslide in the Var canyon (never localised and mapped) located at around 15 km from the coastline. According to Seed et al. (1988), a tidal drawdown associated with a tidal wave resulting from this deep offshore submarine slide has caused a sudden overloading and initiate static liquefaction of loose sand layers present below the harbour embankment. Despite the official scenario (Seed et al. 1988), the origin of the 1979 accident remains a hot topic of debate as evidenced by the number of papers published recently (see for instance Cochonat et al. 1993, Anthony and Julian 1997, Assier-Rzadkiewicz et al. 2000, Sultan et al. 2001, Dan et al. 2007).
Beyond the 1979 accident the aim of this technical note is to present and discuss in terms of failure mechanisms and submarine landslides recent geotechnical and geophysical data acquired to the East of the 1979 slide scar. The present case-study intends i) to improve our understanding of sediment mechanical properties in area prone to failure and ii) to demonstrate the urgent need to develop mitigation procedures to reduce the impact of a possible major landslide in the area.

2. methods

2.1. Swath bathymetry and 3.5 kHz

The swath bathymetric data used in this study were obtained from different oceanographic cruises. The first swath bathymetric survey took place in November 1979, on the R/V Charcot (Pautot 1981). The post-1979 slide swath bathymetric data come from a compilation of SeaBeam, EM1000 and EM300 multibeam sonars. The across-track resolution of the bathymetry depends upon the measured depth. In the present work, the multibeam bathymetry data were gridded at 20 metres.
In this study we also used a 3.5 kHz sub-bottom profiling system which transmit and receive acoustic pulses. When pulse is reflected off the seafloor and layers beneath, it gives seismic profile which provides information on sediment layers, thickness and formations. Seismic profiles display vertical views of the stratigraphy in function of the two-way travel time (TWTT) in milliseconds of the acoustic ray. Conversion to depth in metres is approximate and has been done using a velocity of 1550 m/s. The 3.5 kHz profile provides a vertical resolution of 0.3-0.5 m and a depth penetration that is dependent on the nature of the sediments and the water depth. The 3.5 kHz resolution / penetration ratio is optimum for fine-grained sediments like the ones constituting the Nice shelf. However, the ray path can be affected by gas-rich environments making the interpretation of such very-high resolution seismic more tricky. Several seismic profiles (3.5 kHz) were collected during the PRISME cruise. In this work we discuss and present the three more significant profiles and their stratigraphic interpretation in terms of sediment deformation and slope instabilities (for profiles locations see Figure 2-a).

2.2. Cone penetration testing

In situ geotechnical measurements were carried out using the Ifremer piezocone CPTu (called PENFELD) during the PRISME cruise. The piezocone is designed to work at depths

of up to 6,000 metres. It is equipped with a rod which penetrates the sediment to a depth of 30 metres. The 36mm diameter rod is coiled around a 2.20m diameter drum and is straightened during penetration using the 'coiled tubing' technique. A combination of two special cones (standard CPTu cone and sonic cone) was used in the investigation.
In the Cone Penetration Test a cone on the end of coiled tubing is pushed into the soil layers at a constant rate. The electric cone (10 cm^2) used during the PRISME cruise gives a continuous measurement of the tip resistance (qc), sleeve friction (fs) and excess pore pressure ($\Delta u2$) measured by means of a porous filter located immediately behind the cone (called U2 type cone). The Ifremer CPTu uses a hydrostatically compensated system where the cone load sensor is unaffected by the hydrostatic pressures leading to greater accuracy and sensitivity measurements in soft sediments (Andersen et al. 2008). More details concerning the Ifremer CPTu piezocone are presented in Meunier et al. (2004) and Sultan et al. (2007).
The maximum penetration of the CPTu is 30 m below the seafloor (mbsf). The geometry of the cone penetrometer with tip, sleeve and pore pressure filters follows ISO/DIS 22476-1. During the PRISME cruise the excess pore pressure measurements have failed. The corrected cone resistance qt was therefore calculated from qc and the hydrostatic pore pressure.
The sonic cone is a technology improvement to the standard cone penetrometer. The end of the coiled tubing holds two tips where the first one contains a high-frequency compression wave source (1 MHz) and the second tip the receiver. The distance between receiver and source is equal to 0.07 m (more detail in Sultan et al. 2007). In order to increase the accuracy of the measurement, the compression wave is made over 1000 measurements. As for the standard penetrometer, the sonic CPT is pushed into the sediment layers at a constant rate. A continuous measurement of the P wave velocity and the attenuation is made. During the PRISME cruise, we carried out a total of 9 CPTus and 3 sonic CPT measurements along the Nice slope (Table 1 and Figure 1).

3. Site conditions

3.1. Geological context and seafloor morphology

The Var sedimentary system is located in the Ligurian Sea (NW Mediterranean) and extends from the Nice coastline (SE France) to the continental slope of Corsica (Dan et al. 2007). The Var delta front and slope are cut by major canyons as well as numerous smaller steep-sided valleys and gullies (Anthony and Julian 1997). Several landslides occur at several places along the delta front including the 1979 slide. In Figure 2-a, red dashed polylines indicate the uppermost identified landslides showing horseshoe shaped headwall scars. Moreover, steps (or possible cracks) in the bathymetry are highlighted by light blue dashed polylines in Figure 2-a. Those steps are oriented perpendicular to the slope contours.

3.2. Sub-seafloor seismic data

Figure 2-b through d show 3.5 kHz profiles (CH41001, CH42001 and CH43001) acquired during the PRISME cruise survey (for location see Figure 2-a). CPTus PFM11-S2 and PFM11-S6 locations are projected on the CH41001 profile (Figure 2-b). Three important features can be recognized on the CH41001 profile: 1- in the upper slope, truncated seismic reflections display sedimentary layers outcropping in the head scarp of the lower SE landslide confirming the erosional slide-scars previously interpreted on bathymetry, 2- in depth, the stratigraphic pattern allow to define several seismic reflections between traces 100 and 750 that can be identify by the toplap termination of the internal clinoforms; seaward,

these erosional surfaces are deep-rooted in the gas front, and 3- landward a small morphological step on the seafloor at around 15m water depth topped the major ones of the seismic reflections.
Figure 2-c shows the 3.5 kHz profile CH42001. PFM12-S2 and PFV13-S1 locations are projected on the profile. Two important features can be highlighted from the CH42001 profile: 1- sedimentary layers outcropping in the head scarp of the lower SE landslide confirming once again the morphological interpretation of slope failure presented in Figure 2 and 2- the 1979 landslide scar with residual relatively fresh deposits in the escarpment.
Figure 2-d shows the 3.5 kHz profile CH43001. PFM11-S3 and PFM11-S4 locations are projected on the profile. Three important features can be identified from the CH43001 profile: 1- two seismic reflections between traces 3700 and 3900 converge in a landward direction with a pinch out at 14 m water depth, 2- at that position, a small morphological step imprints the seafloor; its formation seems to be related with these internal surfaces and 3- the presence of possible gas plume or fresh water flow in the water column above the seafloor terrace and associated major seismic reflection. The presence of gas within the shallow prodeltaic sediments of the Var shelf is a common feature in our seismic database (Figure 2). The gas wipeouts observed on seismic sections are blanking the underlying stratigraphic organisation.
Additionally, free gas partially saturating the sediment from the studied shelf was detected by in situ sonic CPT measurements. Low values of Vp (around 750 m/s) were measured at different depths and at the three different sonic CPT sites (Figure 3).

3.3. Shear zones development and clay sensitivity

CPTu piezocone is often used to characterize sediment mechanical properties and lithology (sediment classification) but it can be also used to identify shear zones along which upper mass sediments may move in a slope failure zone. Indeed, Leroueil et al. (1995) and Demers et al. (1999) demonstrated in zones of high shearing where the clay was remoulded that both the penetration tip resistance and the penetration pore pressure were low relative to the undisturbed clay at the same depth. This observation was confirmed by Mahmoud et al. (2000) showing that the CPTu can be used to identify softened zones within a marine clay deposit. For soft marine sediment, shear zones which are characterized by the presence of remoulded sediment are more pronounced on the fs profile (measured over 150 cm^2 of friction sleeve surface) than on the qt profile (measured over 10 cm^2 of tip surface) (Sultan et al. 2007). Obviously, the decrease of the sleeve friction could be also an indication of the clays high sensitivities (Lunne et al. 1997).
For CPTu measurements carried out within the PRISME cruise, the drop in cone resistance and friction was observed at several sites (Figure 4 to Figure 8). The drop in cone resistance was observed between 23 and 28 m for PFM11-S4, 22 and 28 m for PFM11-S5 (Figure 4), 13 and 28 m for PFM12-S1, 18 and 28 m for PFM12-S2 and 17 and 28 m for PFM12-S3 (Figure 6).
The decrease of the friction which could be also an indication of the remoulded state of the sediment was observed for all the 9 sites. By considering a “reference” linear “fs-depth” profile as the one presented in Figure 5 and Figure 7, the supposed shear zones are detected: below 8 m for PFM11-S1, below 5.5 m for PFM11-S2, below 3m for PFM11-S3, below 4 m for PFM11-S4, below 5 m for PFM11-S5, below 9 m for PFM11-S6 (Figure 5), below 4 m for PFM12-S1, below 6.5 m for PFM12-S2 and below 5.5 m for PFM12-S3 (Figure 7).
Piezocone measurements are usually used for estimating sediment undrained shear strength (Su) by using an empirical cone factor called “N_{KT}” (Lunne et al. 1997). The determination of N_{KT} can be done by calibrating qt with a known measured value of Su. For the present study area, the presence of in situ dissolved and free gas (Figure 3) led to gas bubble growth and exsolution during cores recovery and therefore the use of Su values obtained from laboratory tests may induce an important overestimation of N_{KT} values. Figure 9-a shows Su profiles

derived from the piezocone test PFM12-S2 for empirical cone factor N_{KT} of 14 and 20 compared with the Su values obtained from laboratory vane shear tests carried out on core KGMO-06 (core location in Figure 2). Figure 9-a suggests that a N_{KT} value of 14 is appropriate for undisturbed saturated sediments from the study area, however gas exsolution and growth and the associated disrupted sediment structures observed at the base of KGMO-06 (Figure 9-b) may lead to important overestimation of N_{KT}.

3.4. Interpretation of piezocone data and seismic profiles

Comparison between seismic reflections and in situ geotechnical measurements can provide an additional tool to discriminate between plastic shear zones and high sensitive clay. Figure 10 presents a schematic interpretation of 3.5 kHz profile CH41001 showing sediment layers outcropping along the SE slide scar. The important decrease of the friction at PFM11-S6 (at 9 m below the seafloor) fit with a major seismic reflection pointed out on CH41001 profile. The gas front is also blocked at this reflection level.
Figure 11 shows the schematic interpretation of 3.5 kHz profile CH43001. The two seismic reflections pointed out from this profile fit once again with a decrease of the friction at PFM11-S3 and PFM11-S4. Those two reflections are rooted to the morphological step revealed by the bathymetry of the studied area. Although the gas front from the CH43001 profile is deeper than the two seismic reflections, we suspect that it joined the two seismic surfaces at greater depth. The possible gas plume detected in the water column could be an indication of the presence of permeable cracks along and above the termination of the weak surface. Seaward, the 3.5 kHz seismic profiles were not able to penetrate more than 10 to 12 m below the seafloor because the erosional surfaces are deep-rooted in the gas front (Figure 10); therefore it is not possible to correlate deep plastic zones detected by the tip resistance to seismic reflections.

4. Conclusions and implication of potential slide

Different potential shear zones were detected by the 9 in situ piezocone measurements: mainly by sleeve friction for the upper soft sediment and by both friction and tip resistance for deeper stiffer sediment. Shear zones detected owing to the piezocone tip resistance is particularly well expressed between 19 and 28 m on the PFM12-S2. This significant drop of the tip resistance (consequently the shear strength) is characteristic of a “shear zone” resulting from the development of plastic strains and shears. The PFM12-S2 is located closed to one of the most expressed landslide scar (Figure 1). Moreover, almost all CPTu profiles at the border of the plateau are characterized by the presence of shear zones at the base of the CPTu profiles (PFM12-S2, PFM12-S3, PFM11-S4 and PFM11-S5 – see Figure 1 for location).
It is clear that low values of sleeve frictions are also associated to the sensitivity of the clay and from Figure 5 and Figure 7 it is difficult to discriminate between two linked processes: high sensitivity and shear zones. Dan et al. (2007) have already reported the low sleeve friction measured along the Nice coast, which was related to clays high sensitivities and was considered as one of the main causal factors of the 1979 event. Figure 8 presents a blow up of PSM11-S6 data showing that the shear zone which was clearly detected from the sleeve friction can be also seen from the tip resistance profile between 9 and 17 mbsf. Figure 8 confirms what was observed for soft sediment from the Niger delta (Sultan et al. 2007) where the presence of remoulded sediment are more pronounced on the fs profile than on the qt profile.
For the study area, geophysical and geotechnical data demonstrate the presence of discontinuous plastic zones at different depth at least over the first 28 m of subsurface sediment. The dispersion and discontinuity of those shear zones are probably linked to strain and shear localisation (non-uniform stress field). The morphology of the studied plateau

showing the presence of morphological steps and cracks rooted to sub-seafloor shear zones and oriented perpendicular to the slope contours confirms, once again, the presence of localised plastic zones. Acquired data from the study area suggest the start-up of a progressive failure mechanism: “every failure process is, at first, local, with formation of plastic zones, then general (Leroueil, 2001 and Urciuoli et al. 2007)”. The geotechnical and geophysical data acquired during the PRISME cruise do not constrain the timing of deformation and notably the transition from local plastic zones to general failure. This time period can be only predicted by monitoring the displacement rate of the sediment body above the slope failure surface.
Considering the surface of the disturbed shelf (1 km x 0.3 km) and the depth of the identified shear zones (minimum 28 m) the suspected volume which may be involved in a general slope failure can approach the $4x10^6$ m^3. This initial failure volume ($4x10^6$ m^3: half of the 1979 initial slide volume (Mulder et al. 1997) may cause progressive downslope erosion on the upper slope and quickly transform into a debris flow and turbidity current as was the case for the 1979 accident (Mulder et al. 1997). The consequence of such a landslide and turbidity current should urgently be evaluated in terms of generation and propagation of tsunami waves along the SE French coast.

5. References

Andersen, K.H., Lunne, T., Kvalstad, T.J., and Forsberg, C.F. 2008. Deep Water Geotechnical Engineering, *In* Proceedings of The XXIV National Conference of the Mexican Society of Soil Mechanics, Aguascalientes, 26-29 Nov. 2008. Mexican Society of Soil Mechanics, pp. 1-57.

Anthony, E.J., and Julian, M. 1997. The 1979 Var Delta landslide on the French Riviera: A retrospective analysis. Journal of Coastal Research, **13**(1): 27-35.

Assier-Rzadkiewicz, S., Heinrich, P., Sabatier, P.C., Savoye, B., and Bourillet, J.F. 2000. Numerical modelling of a landslide-generated Tsunami: The 1979 Nice event. Pure and Applied Geophysics, **157**(10): 1707-1727.

Cochonat, P., Bourillet, J.F., Savoye, B., and Dodd, L. 1993. Geotechnical characteristics and instability of submarine slope sediments, the Nice slope (N–W Mediterranean Sea). Marine Georesources & Geotechnology, **11**(2): 131-151.

Dan, G., Sultan, N., and Savoye, B. 2007. The 1979 Nice harbour catastrophe revisited: Trigger mechanism inferred from geotechnical measurements and numerical modelling. Marine Geology, **245**(1-4): 40-64.

Demers, D., Leroueil, S., and d'Astous, J. 1999. Investigation of a landslide in Maskinonge, Quebec. Canadian Geotechnical Journal, **36**(6): 1001-1014.

Leroueil, S., Demers, D., La Rochelle, P., Martel, G., and Virely, D. 1995. Practical use of the piezocone in eastern Canada clays. *In* CPT’95, Proceedings of the International Symposium on Cone Penetration Testing, Linköping, 4-5 October 1995. Swedish Geotechnical Institute, pp. 515–521.

Leroueil, S. 2001. Natural slopes and cuts: movement and failure mechanisms. Geotechnique, **51**(3): 197-243.

Lunne, T., Robertson, P.K., and Powell, J.J.M. 1997. Cone Penetration Test in Geotechnical Practice. Blackie Academic and Professional, UK.

Mahmoud, M., Woeller, D., and Robertson, P.K. 2000. Detection of shear zones in a natural clay slope using the cone penetration test and continuous dynamic sampling. Canadian Geotechnical Journal, **37**(3): 652-661.

Meunier, J., Sultan, N., Jegou, P, and Harmegnies F. 2004. First tests of Penfeld: a new seabed penetrometer. *In* Proceedings of The Fourteenth International Offshore and Polar Engineering Conference, pp. 338-345.

Mulder, T., Savoye, B., and Syvitski, J.P.M. 1997. Numerical modelling of a mid-sized gravity flow: the 1979 Nice turbidity current (dynamics, processes, sediment budget and seafloor impact). Sedimentology, **44**: 305–326
Pautot, G. 1981. Carte morphologique de la Baie des Anges, Modèle d'instabilité de pente continentale. Oceanologica Acta, **4**(2): 203-212.
Seed, H.B., Seed, R.B., Schlosser, F., Blondeau, F., and Juran, I., 1988. The Landslide at the Port of Nice on October 16, 1979. University of California, College of Engineering, Report No. UCB/EERC-88/10.
Sultan, N., Cochonat, P., Bourillet, J.F., and Cayocca, F. 2001. Evaluation of the risk of marine slope instability: A pseudo-3D approach for application to large areas. Marine Georesources & Geotechnology, **19**(2): 107-133.
Sultan, N., Voisset, M., Marsset, B., Marsset, T., Cauquil, E., and Colliat, J.L. 2007. Potential role of compressional structures in generating submarine slope failures in the Niger Delta. Marine Geology, **237**(3-4): 169-190.
Urciuoli, G., Picarelli, L., and Leroueil, S. 2007. Local soil failure before general slope failure, Geotechnical and Geological Engineering, **25**: 103-122.

Tables

#	Lat	Long	Tool	Water Depth (m)	Penetration (m)
PFM11-S4	43.64850	7.22575	CPTu	21	28
PFM11-S3	43.64826	7.22526	CPTu	21	28
PFM11-S2	43.64630	7.22247	CPTu	15	28
PFM11-S5	43.64743	7.22640	CPTu	24	28
PFM11-S1	43.64628	7.22110	CPTu	20	28
PFM11-S6	43.64522	7.22383	CPTu	19	28
PFM12-S1	43.64265	7.21113	CPTu	20	28
PFM12-S2	43.64338	7.21938	CPTu	19	28
PFM12-S3	43.64422	7.22177	CPTu	19	28
PFV13-S1	43.64388	7.21922	CPTu	19	28
PFV13-S2	43.64548	7.22438	Sonic CPT	15	28
PFV13-S3	43.64760	7.22627	Sonic CPT	17	28

Table 1. Coordinates and characteristics of CPTus and sonic CPT locations.

Figures

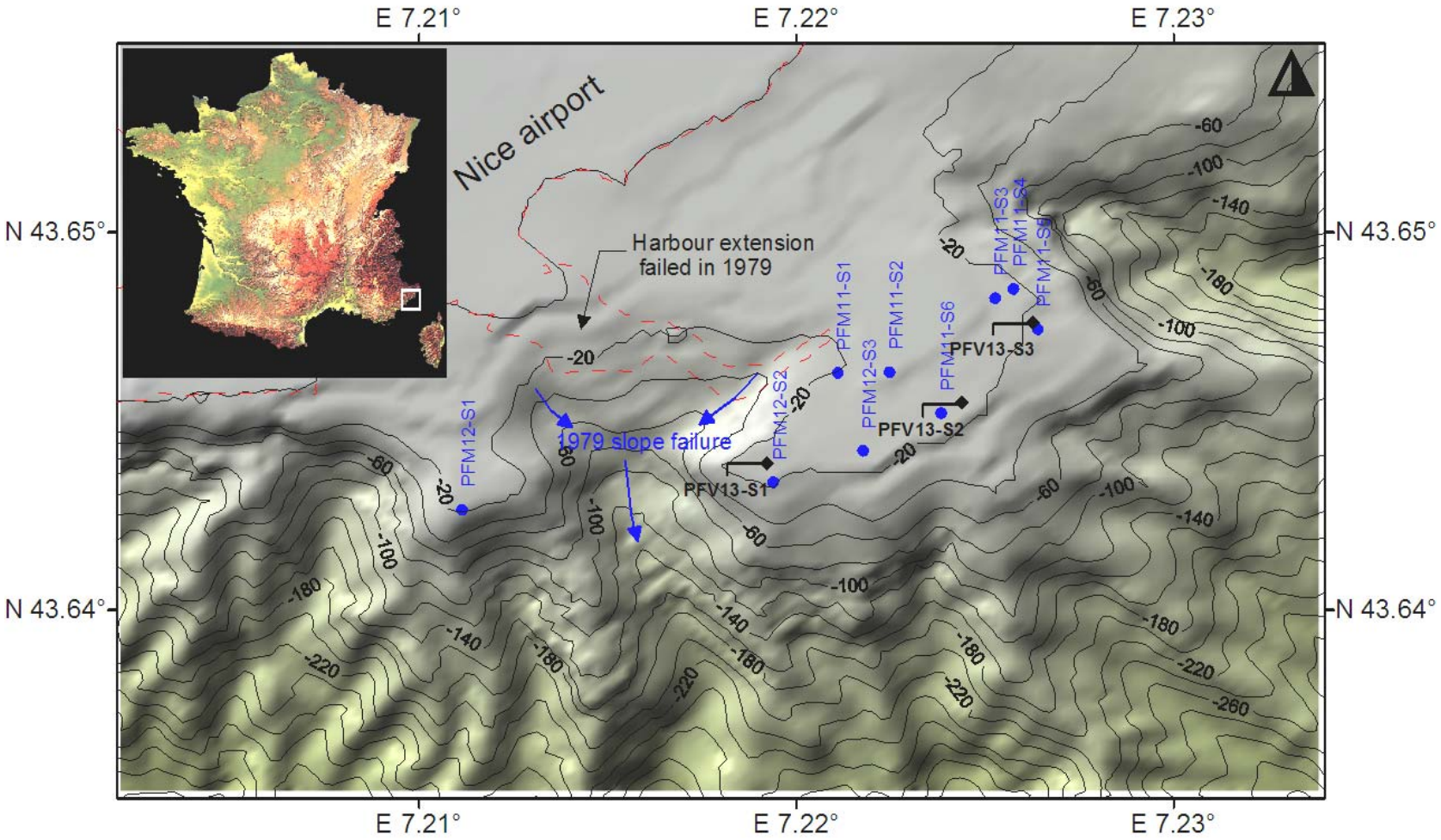

Figure 1. CPTu (PFM) and sonic CPT (PFV) locations projected on shaded bathymetric map. The failed harbour extension and the 1979 slope failure are also indicated.

(a)

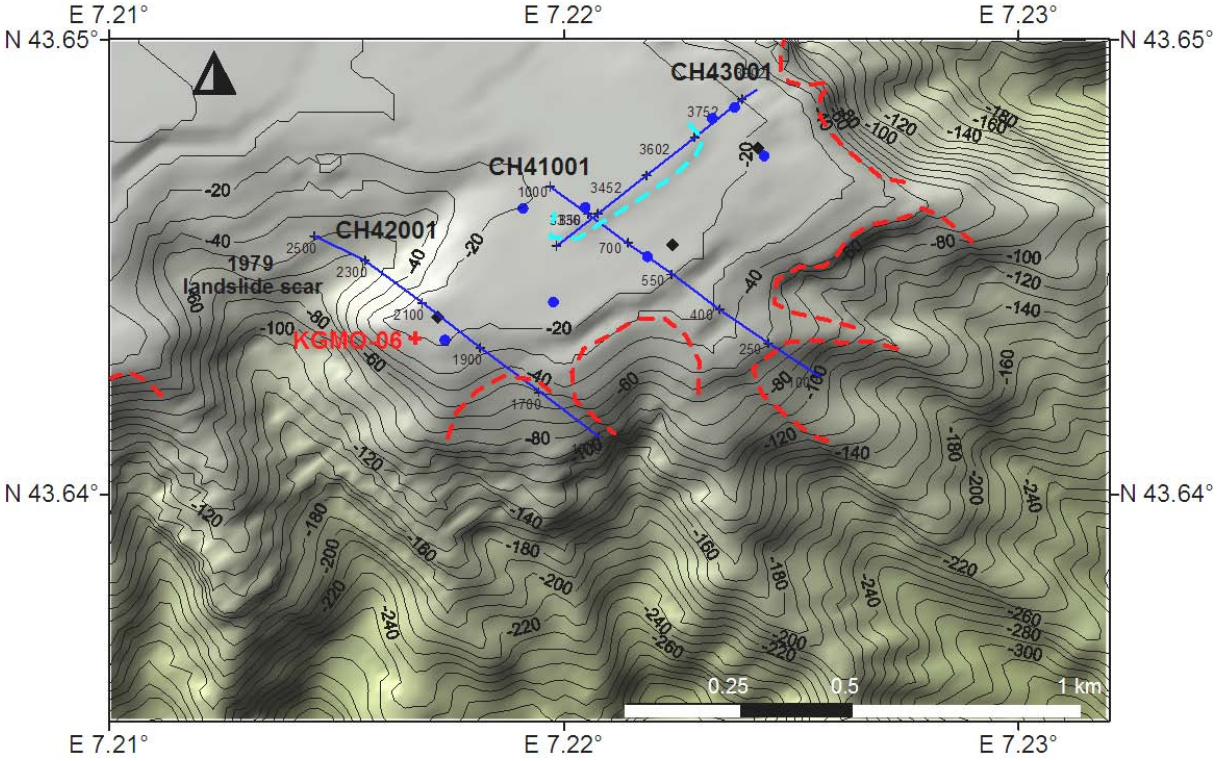
E 7.21°
E 7.22°
E 7.23°
N 43.65°
N 43.64°
CH43001
CH41001
CH42001
1979
landslide scar
KGMO-06
0.25
0.5
1 km

(b)

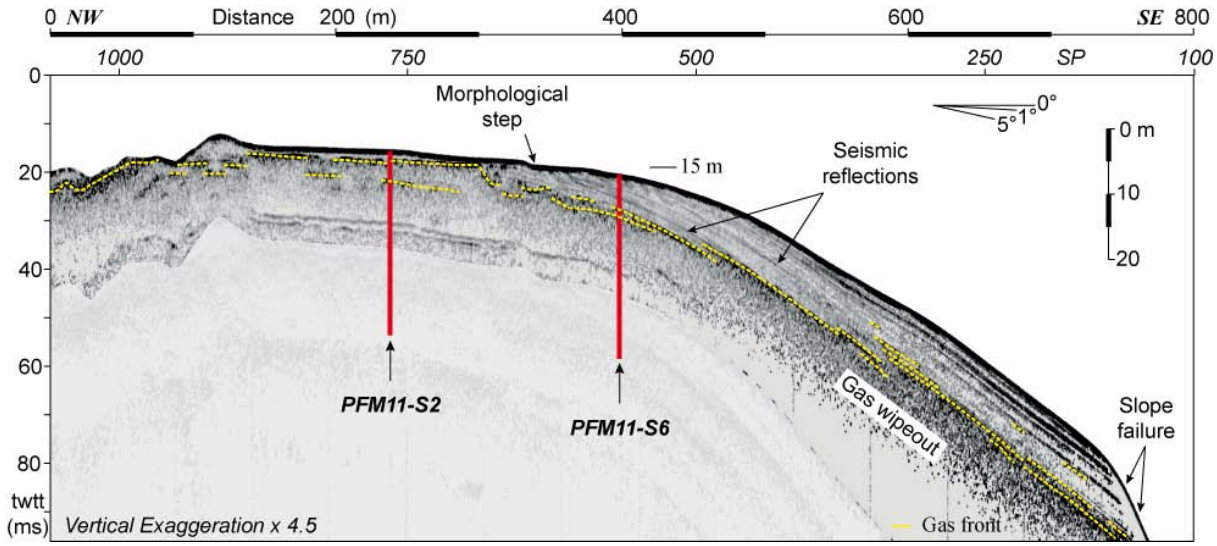
0 NW
Distance 200 (m)
400
600
SE 800
1000
750
500
250
SP
100
Morphological step
15 m
Seismic reflections
0°
5°
1°
0 m
10
20
PFM11-S2
PFM11-S6
Gas wipeout
Slope failure
twtt (ms)
Vertical Exaggeration x 4.5
Gas front

(c)

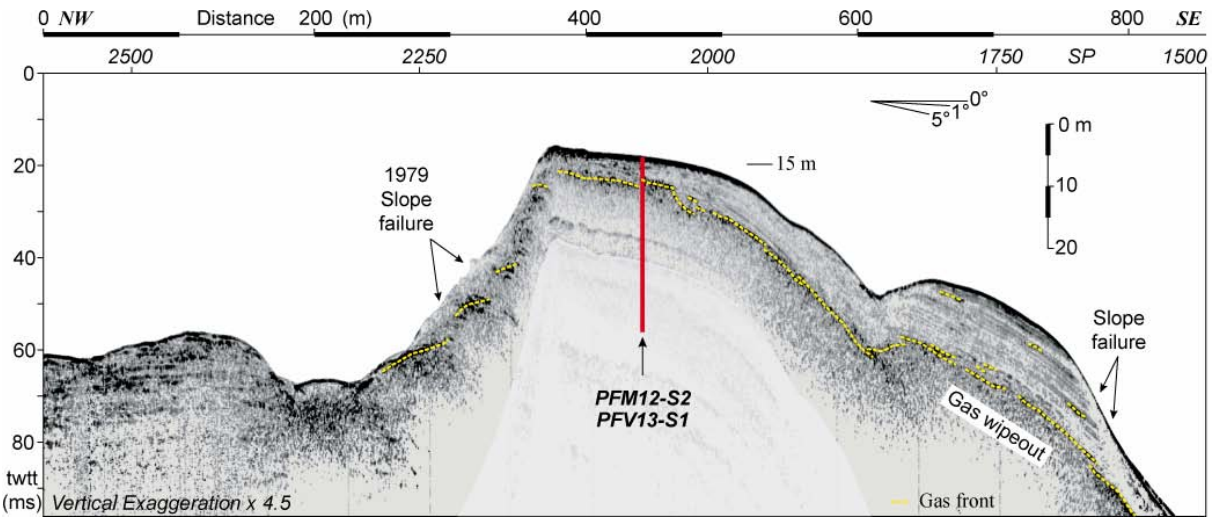

(d)

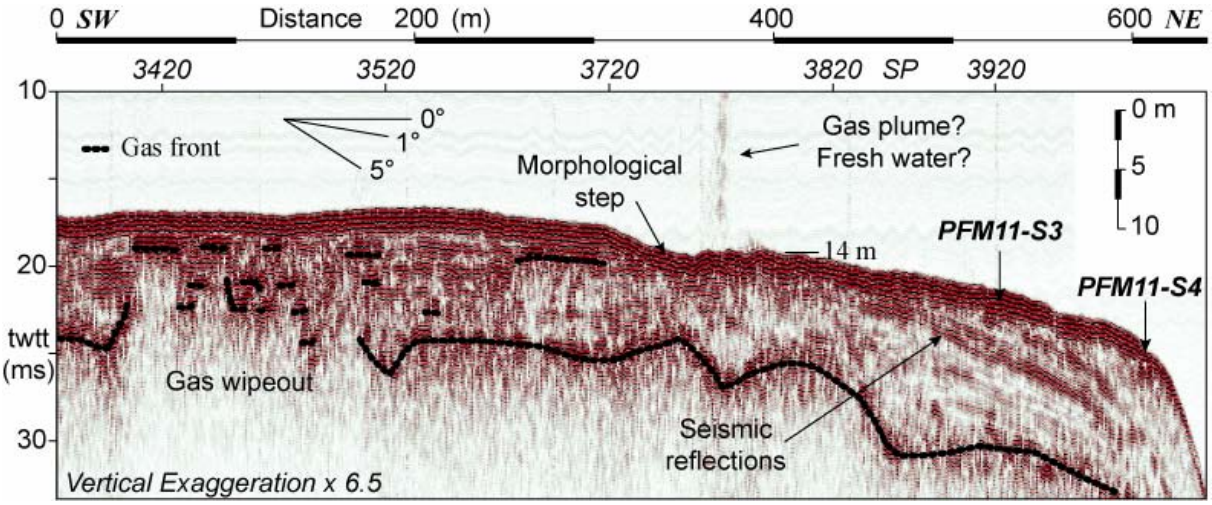

Figure 2. a) Location of three 3.5 kHz profiles acquired during the PRISME cruise. Red dashed polylines indicate the uppermost landslides and light blue dashed polylines highlight morphological steps. b) profile CH41001 showing a slope failure to the SE and a major seismic reflection at around 6 mbsf (Vertical exaggeration: x 4.5). c) profile CH42001 showing the upper part of a slope failure to the SE initiated at a water depth of 45 m. The 1979 scar and deposit can be also observed to the NW of the profile (Vertical exaggeration: x 4.5). d) Profile CH43001 showing the presence of two seismic reflections to the NE at the edge of the slope (Vertical exaggeration: x 6.5). The two major seismic reflections fit with small seafloor morphological steps. A gas plume or fresh water flow can be observed in the water column above the morphological depression (trace: 3660-3670).

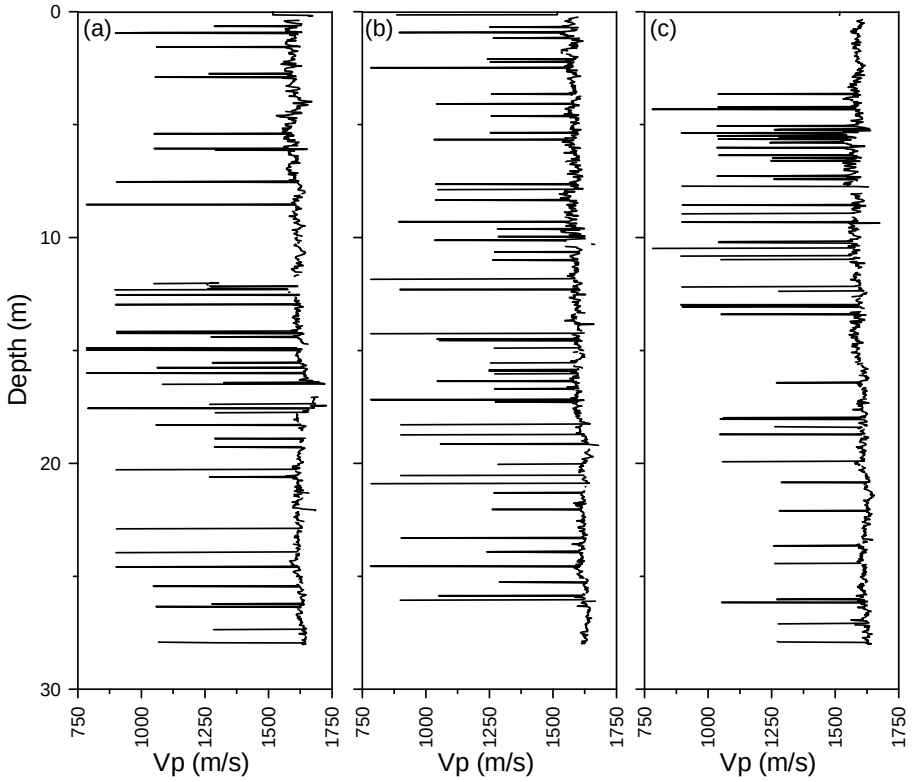

Figure 3. The presence of the free gas partially saturating the sediment from the Nice plateau was detected thanks to in situ sonic CPT measurements. Low values of Vp (around 750 m/s) were measured at different depths of the three different sonic CPT sites a) PV13-S1, b) PV13-S2 and c) PV13-S3 (for location see Figure 1).

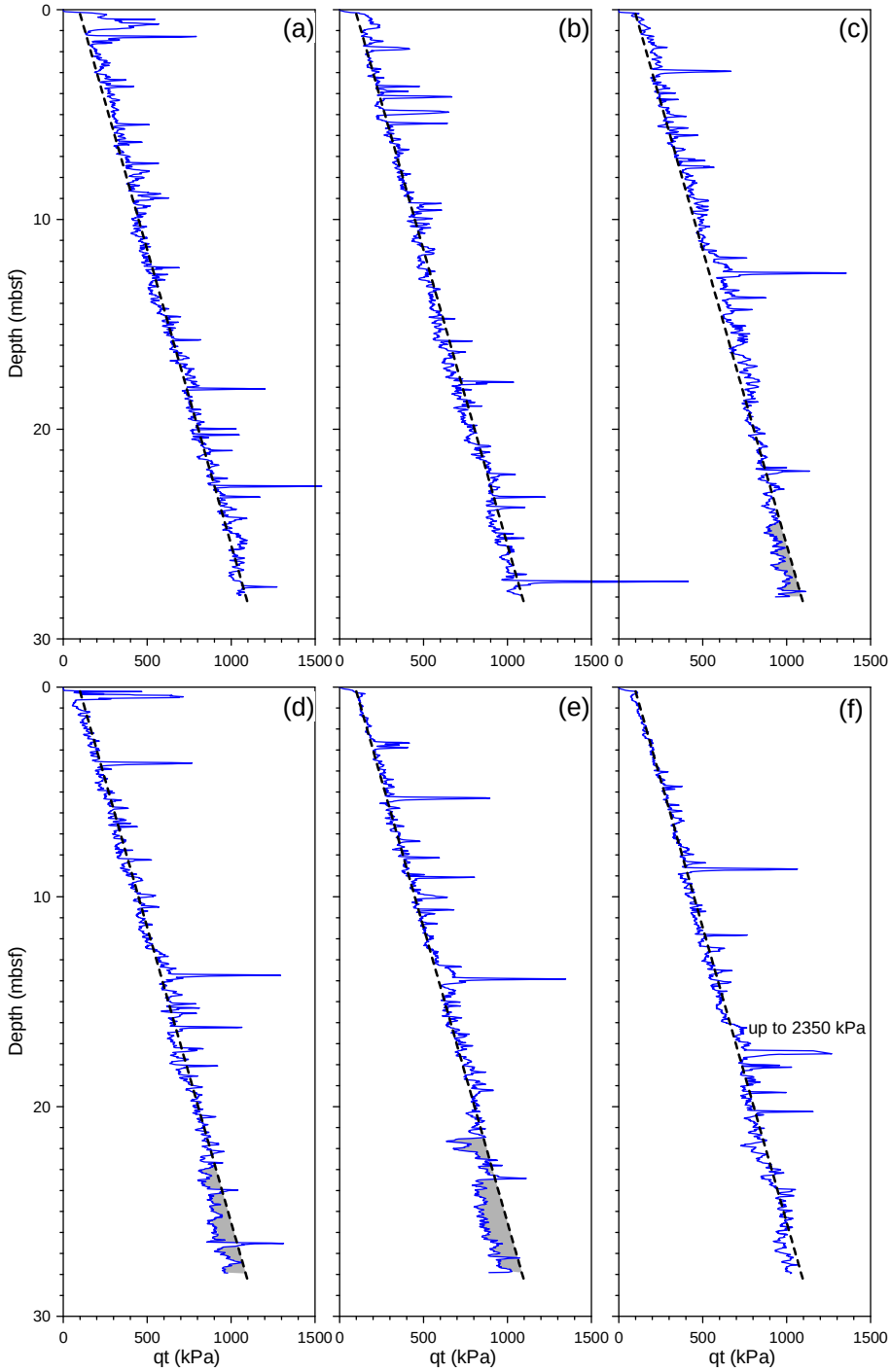

Figure 4. Corrected tip resistance qt versus depth from a) PFM11-S1; b) PFM11-S2; c) PFM11-S3; d) PFM11-S4; e) PFM11-S5 and f) PFM11-S6. For the 6 sites the presence of coarse sediments is shown by high values the tip resistance. Shaded areas indicate significant decrease of the corrected tip resistance.

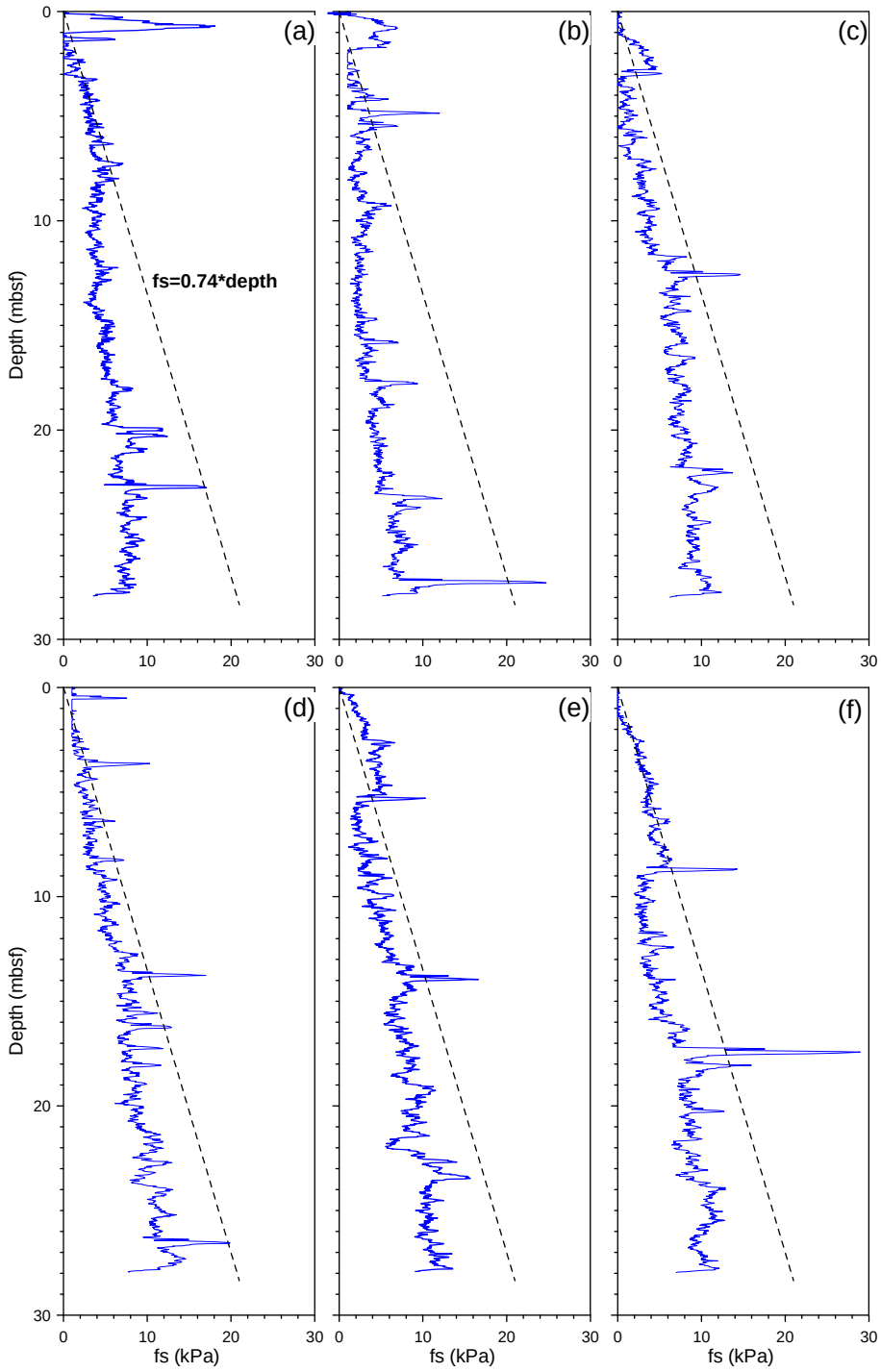

Figure 5. Friction versus depth from a) PFM11-S1; b) PFM11-S2; c) PFM11-S3; d) PFM11-S4; e) PFM11-S5 and f) PFM11-S6. For the 6 sites the presence of coarse sediments is shown by high values of friction.

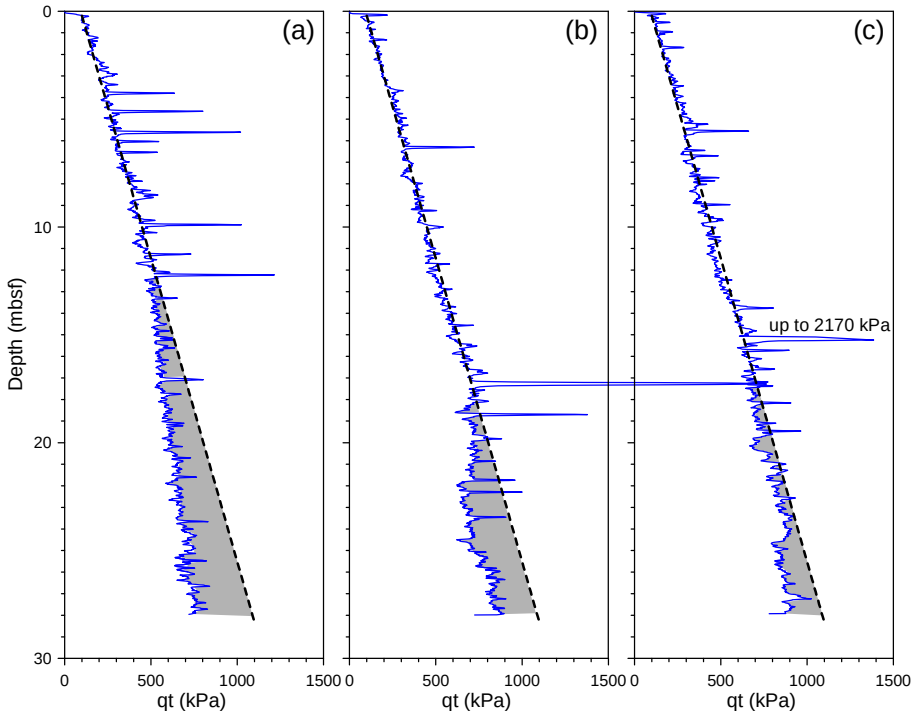

Figure 6. Corrected tip resistance qt versus depth from a) PFM12-S1; b) PFM12-S2; c) PFM12-S3. For the 3 sites the presence of coarse sediments is shown by high values the tip resistance. Shaded areas indicate significant decrease of the corrected tip resistance.

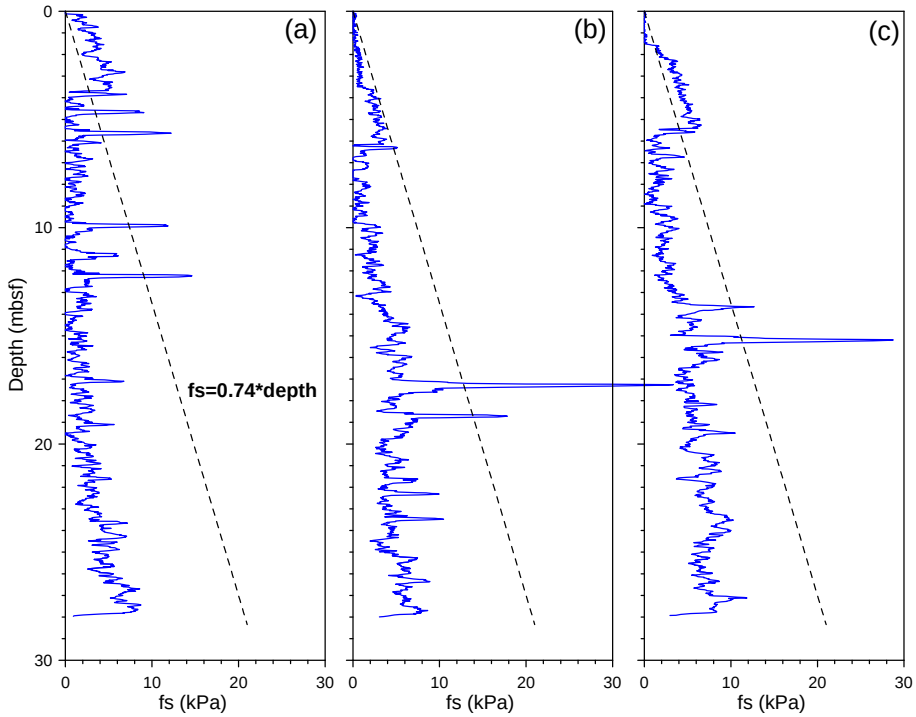

Figure 7. Friction versus depth from a) PFM12-S1; b) PFM12-S2; c) PFM12-S3. For the 3 sites the presence of coarse sediments is shown by high values of friction.

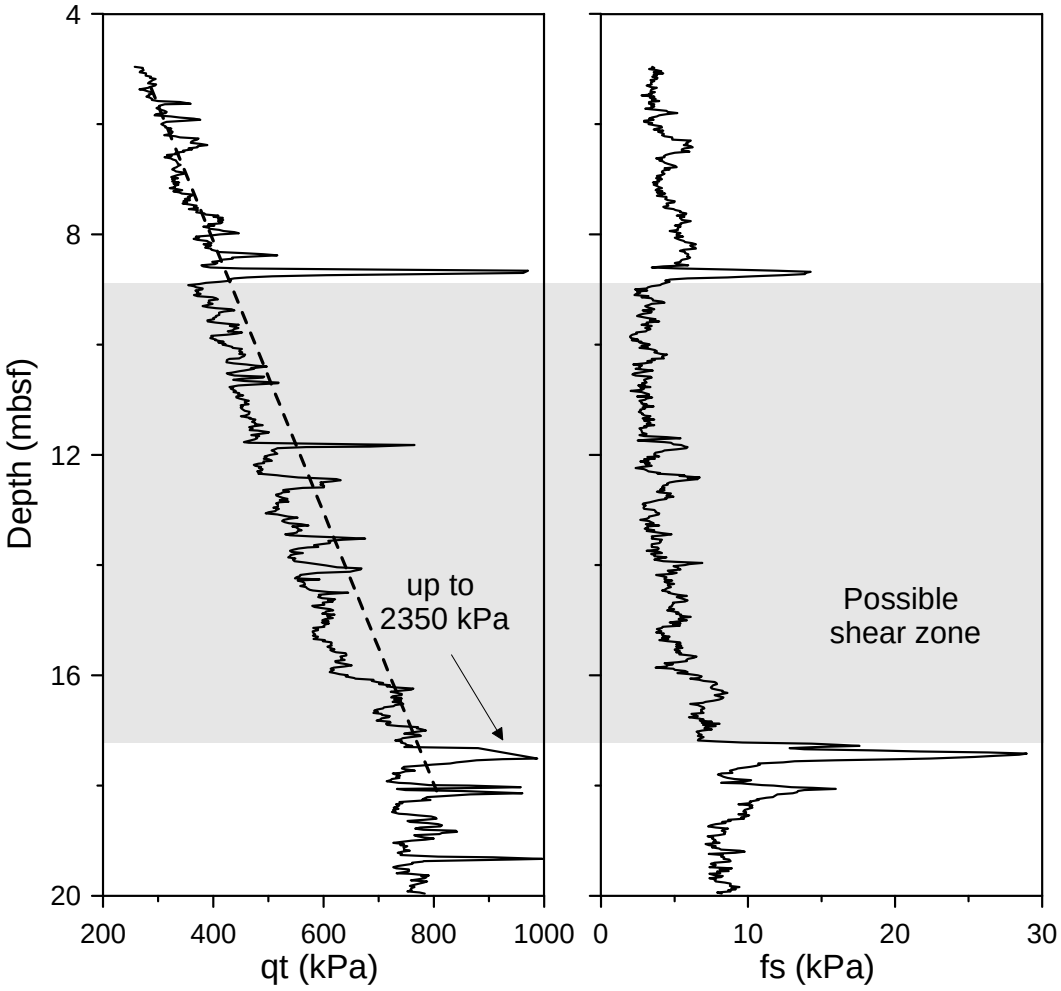

Figure 8. PFM11-S6: Blow up of the corrected tip resistance and friction versus depth. The shear zone which was clearly detected from the friction can be also seen from the tip resistance profile between 9 and 17 mbsf.

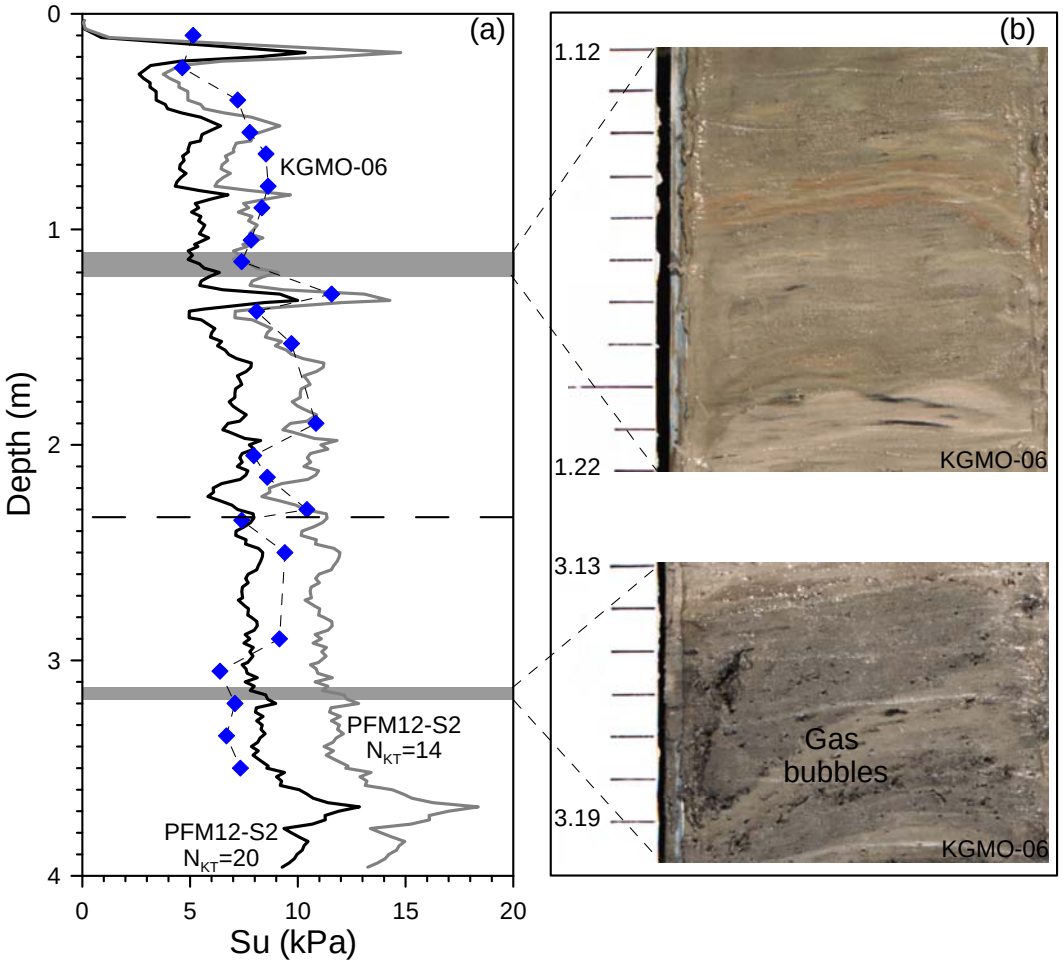

Figure 9. a) Undrained shear strength, Su, profiles derived from the piezocone test PFM12-S2 for empirical cone factor N_{KT} of 14 and 20 compared with the Su values measured from laboratory vane shear tests. b) Photos of selected intervals from core KGMO-06 showing the vertical heterogeneity of the sediment. Note the disrupted sediment structures in the lower part of KGMO-06 and gas bubbles that exsolved during core retrieval.

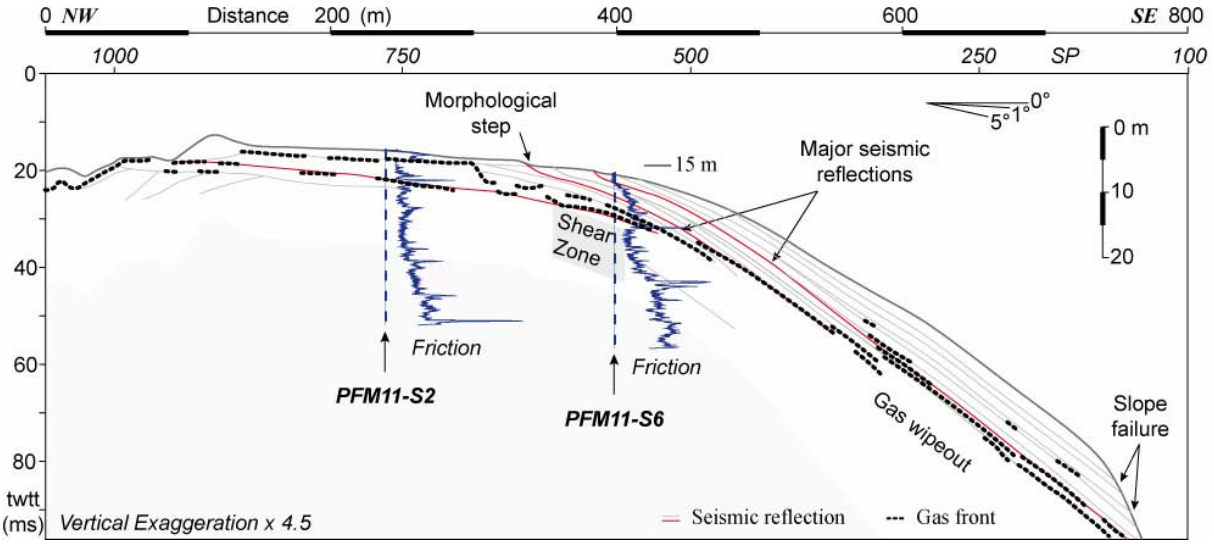

Figure 10. Schematic interpretation of 3.5 kHz profile CH41001 (Figure 2-b) showing sediment layers outcropping along the SE slide scar. The important decrease of the friction at PFM11-S6 fits with a major seismic reflection (Vertical exaggeration: x 4.5).

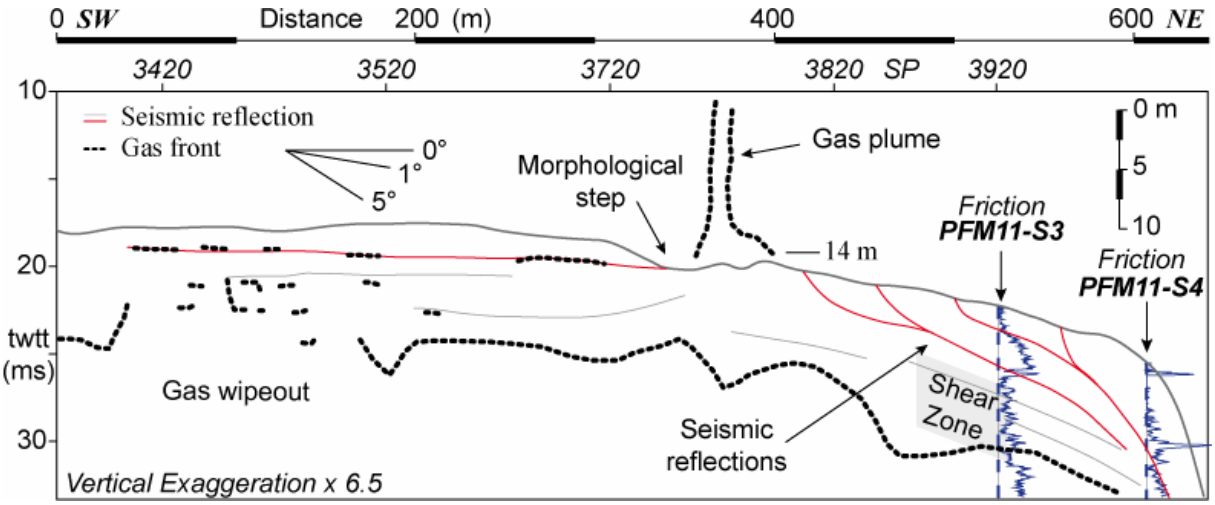

Figure 11. Schematic interpretation of 3.5 kHz profile CH43001 (Figure 2-d) showing two seafloor morphological steps rooted at the top of two seismic reflections. Internal seismic reflections correspond to an important decrease of the friction at PFM11-S3 and a less significant decrease at PFM11-S4. Above the SW step a gas plume or fresh water flow is detected in the water column (Vertical exaggeration: x 6.5).